Inorg. Chem. **1997,** *36,* 1689−1693

Synthesis and Characterization of $Cs_5Sb_8S_{18}(HCO_3)$: A New Layered Phase Containing Interstitial Cations and Anions

George L. Schimek and Joseph W. Kolis*

Department of Chemistry, Clemson University, Clemson, South Carolina 29634-1905

Received April 3, 1996⊗

A new pseudoternary phase, $Cs_5Sb_8S_{18}(HCO_3)$, was prepared from supercritical ammonia at 160 °C over 4 days using stoichiometric quantities of Cs_2CO_3, Sb_2S_3, and S_8. Red parallelepipeds of the title phase crystallize in the centrosymmetric monoclinic space group $C2/c$, with $a = 27.064(3)$ Å, $b = 11.634(4)$ Å, $c = 12.642(3)$ Å, $\beta = 97.45(2)°$, and $Z = 4$. The compound has a layered structure, with the layers formed from ribbons of condensed ψ-SbS_4 trigonal bipyramids linked via S_3^{2-} chains, and both Cs^+ and HCO_3^- ions between the layers, giving rise to the formula $Cs_5Sb_8S_{12}(S_3)_2(HCO_3)$. Each layer is approximately 10 Å thick, with two layers per unit cell. The condensation of the group 15/16 building blocks into ribbons is the result of a combination of edge- and vertex-shared antimony(III) sulfide pseudo trigonal bipyramids. In this phase, the S_3 chains always link adjacent ribbons via apical coordination sites on the antimony atoms. The open cavities created by the linking trisulfide dianions between neighboring ribbons accommodate the antimony lone pairs and two unique cesium cations. A third cesium cation is located between layers. Unique to this compound, the anionic antimony sulfide layers are separated not only by cesium cations but also by bicarbonate anions. Results derived from infrared spectroscopy, diffuse reflectance, bond valence sums, and magnetic susceptibility measurements support the formulation of this compound as an electron-precise, wide-bandgap material. Thermal stability studies of $Cs_5Sb_8S_{18}(HCO_3)$ are also discussed.

Introduction

The investigation of anionic polymers of the main group elements, or Zintl phases, is currently of great interest. In particular, the Cs−Sb−S system is structurally quite rich. The first compounds to be reported about 20 years ago were $CsSbS_2$,[1] $Cs_2Sb_4S_7$,[2] $Cs_2Sb_8S_{13}$,[3] and $Cs_4Sb_{14}S_{23}$.[4] Almost a decade passed before the synthesis and characterization of four more members in this system: $Cs_3Sb_5S_9$,[5] $Cs_6Sb_{10}S_{18}\cdot 1.2H_2O$,[6] and $Cs_2Sb_4S_8$ and $CsSbS_6$.[7]

The structural diversity observed in these cesium antimony sulfides is derived, in part, from the varied condensation of one or more of the three basic building units of Sb(III)-S frameworks: SbS_3 trigonal pyramids, ψ-SbS_4 pseudo trigonal bipyramids, and ψ-SbS_5 octahedra. Another structural feature in two of the more recent members is the inclusion of S_y chains ($y = 2, 5$).[7] These phases all have one- or two-dimensional frameworks with the cesium cations located between the antimony sulfide chains, columns, or layers. As of yet, no extended three-dimensional antimony sulfide framework containing cesium is known. However, the recent syntheses of $[N(CH_3)_4]Sb_3S_5$,[8] $[CH_3NH_3]_2Sb_8S_{13}$,[9] $[H_3N(CH_2)_3NH_3]Sb_{10}S_{16}$,[10] and $[Mn(NH_3)_6]Sb_6S_{10}$[11] indicate that such three-dimensional frameworks with bulky cations are possible.

All the previously reported Cs−Sb−S compounds were synthesized using relatively low-temperature routes, such as fluxes, or variations on the solventothermal methods described by Rabenau.[12] Efforts in this laboratory have centered upon the use of supercritical amines to form novel quaternary phases. A rich structural chemistry in the Cs−M−Sb−S system (M = Cu, Ag) has unfolded, involving, in particular, one-dimensional phases such as $Cs_3Ag_2Sb_3S_8$ and Cs_2AgMS_4[13] (M = As, Sb) and two-dimensional phases such as $CsAgSb_4S_7$, $Cs_2Ag_3Sb_3S_7$,[14] $CsCu_2SbS_3$,[15] and $Cs_2Cu_2Sb_2S_5$.[16] In the course of our investigation of these systems in supercritical ammonia, the pseudoternary phase, $Cs_5Sb_8S_{18}(HCO_3)$, was discovered. It contains antimony sulfide ribbons linked by S_3^{2-} chains to form layers. Both cesium cations and bicarbonate anions are located between these layers. In this paper, the synthesis, physical properties, and structure of this compound are discussed.

Experimental Section

General Techniques. IR spectra of samples in KBr pressed pellets were recorded on either a Nicolet Magna-IR 550 near-IR spectrometer or a Bomem MB-102 FTIR spectrometer equipped with CsI optics. KBr (Harshaw Chemical Co., IR quality) was dried by melting it in a platinum crucible and immediately storing it in a drybox. The samples were prepared in a drybox with freshly ground KBr and then thoroughly purged in the IR sample port before collecting spectra. An optical bandgap for the title phase was determined from room-temperature diffuse reflectance measurements over the 200−800 nm range on a Shimadzu UV3100 spectrophotometer equipped with an integrating sphere attachment. Barium sulfate was used as the reflectance standard. The reflectance data were converted to relative absorption units using

---

⊗ Abstract published in *Advance ACS Abstracts*, March 15, 1997.

(1) Kanishcheva, A. S.; Mikhailov, Y. N.; Kuznetsov, V. G.; Batog, V. N. *Dokl. Akad. Nauk SSSR* **1980**, *251* (3), 603.

(2) Dittmar, V. G.; Schäfer, H. *Z. Anorg. Allg. Chem.* **1978**, *441*, 98.

(3) Volk, K.; Schäfer, H. *Z. Naturforsch.* **1979**, *34B*, 1637.

(4) Kanishcheva, A. S.; Kuznetsov, V. G.; Mikhailov, Y. N.; Batog, V. N.; Skorikov, V. M. *Zh. Strukt. Khim.* **1980**, *21* (5), 136.

(5) Sheldrick, W. S.; Häusler, H.-J. *Z. Anorg. Allg. Chem.* **1988**, *561*, 149.

(6) Parise, J. B. *J. Chem. Soc., Chem. Commun.* **1990**, *22*, 1533.

(7) McCarthy, T. J.; Kanatzidis, M. G. *Inorg. Chem.* **1994**, *33*, 1205.

(8) Parise, J. B. *Science* **1991**, *251*, 293.

(9) Wang, X.; Liebau, F. *J. Solid State Chem.* **1994**, *111*, 385.

(10) Wang, X. *Eur. J. Solid State Inorg. Chem.* **1995**, *32*, 303.

(11) Young, D. M.; Schimek, G. L.; Wilcenski, S. M.; Kolis, J. W. *Inorg. Chem.*, submitted.

(12) Rabenau, A. *Angew. Chem., Int. Ed. Engl.* **1985**, *24*, 1026.

(13) Wood, P. T.; Schimek, G. L.; Kolis, J. W. *Chem. Mater.* **1996**, *8*, 721.

(14) Jerome, J. E.; Schimek, G. L.; Pennington, W. T.; Kolis, J. W. Unpublished results.

(15) Jerome, J. E.; Pennington, W. T.; Kolis, J. W. *Inorg. Chem.* **1994**, *33*, 1733.

(16) Jerome, J. E.; Schimek, G. L.; Kolis, J. W. Unpublished results.

S0020-1669(96)00359-X CCC: $14.00

Table 1. X-ray Crystallographic Data

formula	$Cs_5Sb_8S_{18}(HCO_3)$	V (Å^3)	3947(1)
fw	2276.6	calcd density (g/cm^3)	5.658
space group, Z	$C2/c$ (No. 15), 4	μ (mm^{-1})	10.90
a (Å)	27.064(3)	temp (°C)	−100
b (Å)	11.634(4)	λ (Å)	0.7107
c (Å)	12.642(3)	R,[a] R_w[b]	0.0425,
β (deg)	97.45(2)		0.0431

[a] $R = \sum||F_o| - |F_c||/\sum|F_o|$. [b] $R_w = [\sum w\{|F_o| - |F_c|\}^2/\sum w|F_o|^2]^{1/2}$; $w = 1/\sigma^2\{|F_o|\}$.

the Kubelka–Munk function.[17] The magnetic properties of powders of the title phase were examined with a MPMS Quantum Design SQUID magnetometer. The samples were loaded into quartz baskets and data collected from 4 to 300 K. The data were subsequently corrected for the diamagnetic contribution of the quartz holder. The thermal stability of the title phase was examined with a TA Instruments Thermal Analyst 2000 equipped with a 910 differential scanning calorimeter. Samples were loaded into aluminum pans and hermetically sealed in the drybox. The samples were referenced against a blank aluminum pan and heated from 300–720 K under a helium gas purge. Elemental analyses (C, H) were performed by Atlantic Microlab, Atlanta, GA. X-ray powder diffraction studies were performed on microcrystalline samples at room temperature using a Scintag XDS 2000 $\theta-\theta$ diffractometer equipped with Cu Kα radiation (λ = 1.540 562 Å).

Synthesis. The title phase, $Cs_5Sb_8S_{18}(HCO_3)$, was prepared using methods similar to those first reported by Rabenau,[12] from stoichiometric quantities (10:16:3 mole ratio) of Cs_2CO_3 (96 mg, Aldrich, 99.9%), Sb_2S_3 (182 mg, Strem, 98%), and S_8 (3 mg, Mallinckrodt, 99.9%). The reagents were placed in fused-silica tubes (5 mm i.d., 7 mm o.d., 1.2 cm^3 sealed volume) under an argon atmosphere in a Vacuum Atmospheres drybox. The tubes were subsequently evacuated (~10^{-3} torr), and approximately 0.5 mL (40% fill) of NH_3 was distilled onto the reagents. The tubes were flame-sealed after freezing the solvent and then thawed to give dark purple solutions and some insoluble reagents. The fused-silica tubes were placed in a high-pressure autoclave, an argon counterpressure of 3200 psi applied, and the reaction vessel heated at 160 °C for 4 days. After cooling, the liquid NH_3 was slightly yellow to colorless, indicating that few reagents remained in solution. The title compound formed as transparent, bright red, fibrous needles in nearly quantitative yield. Removal of the solvent produced a dark red-brown powder. IR (KBr pellet, cm^{-1}): 3142 (w), 1645 (w), 1625 (w), 1400 (m), 1126 (s), 996 (s), 739 (sh), 659 (m), 614 (sh), 533 (sh), 471 (sh), and 423 (sh). Anal. Calcd for $CHO_3S_{18}Sb_8Cs_5$: C, 0.53; H, 0.04. Found: C, 0.80; H, 0.36. Growth of samples large enough for single-crystal X-ray diffraction studies was promoted by the presence of copper metal.

Crystallography. A single crystal measuring 0.03 × 0.05 × 0.13 mm^3 was isolated under Nujol after decanting the cooled ammonia solution. It was mounted in a capillary with quick-drying epoxy. A Rigaku AFC7R four-circle diffractometer equipped with graphite-monochromated Mo Kα radiation (λ = 0.710 73 Å) was utilized. Lattice parameters were derived from 25 randomly located and centered reflections with a 2θ range of 12.0–35.6°. Three standard reflections were measured every 100 reflections and showed negligible variation in intensity (<±1.2%) throughout the data collection. An ω-scan mode (16°/min with ≤3 rescans) was utilized. Data were collected from 4– to 50° in 2θ in the $h,k,\pm l$ quadrant with $h + k = 2n$. The number of reflections measured was 3754, of which 3671 were unique (R_{int} = 0.077) and 1724 were observed with $I > 2\sigma(I)$. The intensity data were corrected for Lorentz and polarization effects. Further details are included in Table 1.

The space group, $C2/c$, was chosen on the basis of the centering condition and the systematic absences of $h0l$, h, $l = 2n + 1$, and $00l$, $l = 2n + 1$. The structure was solved by direct methods, SHELXS-86,[18] and refined on $|F|$ by full-matrix, least-squares techniques with TEXSAN[19] and SHELXTL-PLUS.[20] Scattering factors for all atoms were taken from the source programs utilized. An empirical ψ-scan absorption correction (0.65–1.00) was applied. All cesium, antimony, and sulfur atom thermal parameters were refined anisotropically. Oxygen, carbon, and hydrogen atom thermal parameters were refined isotropically or fixed. The number of variables refined was 150. Maximum and minimum residual electron densities were 1.4 and −2.8 e/Å^3. Charge considerations necessitate a monocharged interlayer anion at full occupancy (*vide infra*). All least-squares refinements with a half-occupied carbonate anion diverged.

Table 2. Positional and Isotropic Thermal Parameters (Å^2) for $Cs_5Sb_8S_{18}(HCO_3)$

atom	x	y	z	B(eq)[a]
Cs1	0.13043(6)	0.7951(2)	0.7144(1)	2.10(4)
Cs2	0.06237(6)	0.1962(2)	0.5433(1)	2.22(4)
Cs3	$^1/_2$	0.0502(3)	$^3/_4$	5.4(1)
Sb1	0.25796(6)	0.1081(1)	0.6612(1)	1.22(4)
Sb2	0.30812(6)	0.9004(1)	0.8815(1)	1.24(4)
Sb3	0.35413(6)	0.8910(1)	0.6148(1)	1.29(4)
Sb4	0.18999(6)	0.1051(2)	0.9318(1)	1.35(4)
S1	0.2875(2)	0.1024(5)	0.8871(4)	1.3(1)
S2	0.3556(2)	0.9064(5)	0.0713(4)	1.6(1)
S3	0.3868(2)	0.9362(5)	0.8041(4)	1.3(1)
S4	0.2559(2)	0.9028(6)	0.6678(4)	1.5(1)
S5	0.1620(2)	0.0975(6)	0.7373(4)	1.5(1)
S6	0.1949(2)	0.8985(6)	0.9701(4)	1.6(1)
S7	0.0925(2)	0.9226(5)	0.4498(5)	2.0(2)
S8	0.0545(2)	0.7975(6)	0.3603(5)	2.2(2)
S9	0.0568(3)	0.6460(6)	0.4466(6)	2.5(2)
O1	0.0348(6)	0.784(2)	0.811(1)	2.6(3)
O2	0.013(1)	0.053(3)	0.719(3)	2.6
C1	0	0.841(3)	$^3/_4$	0.8(5)
H1	0.032	0.070	0.166	6.3

[a] The isotropic thermal parameter is defined as $(8\pi^2/3)\{\sum_i\sum_j(U_{ij}a_i{}^*a_j{}^*\vec{a}_i\cdot\vec{a}_j)\}$ where the summations of i and j range from 1 to 3.

The isotropic thermal parameter of Cs3 is unusually large, and the general positional and thermal behavior of the bicarbonate anion is also suspect (*vide infra*). These atoms reside on or near the 2-fold rotation axes. Thus refinements in Cc were undertaken. Unfortunately, the space group change did not resolve the problems noted for Cs3 and the bicarbonate anion. In fact, large correlation coefficients were observed resulting in oscillatory motion of the heavy-atom positions and isotropic thermal parameters. This behavior could not be dampened and likely indicates that the majority of the atoms are related by the symmetry imposed by $C2/c$. Thus the structural results are reported in the centrosymmetric space group. Crystallographic details are given in Table 1, and positional parameters with isotropic thermal parameters are listed in Table 2.

Structural Description

$Cs_5Sb_8S_{18}(HCO_3)$, shown in Figure 1, has two layers per unit cell, related by the centering operator. Each layer contains condensed antimony sulfide ribbons which repeat infinitely along [001]. A fragment of the anionic antimony sulfide framework exhibiting the two modes of pseudo trigonal bipyramidal condensation is shown in Figure 2. Two edges of the ψ-SbS_4 trigonal bipyramid of Sb1 are shared with two other ψ-SbS_4 bipyramids (Sb2 and Sb4), and the remaining apical coordination site is a vertex-shared sulfur (S6) bonding to another ψ-SbS_4 (Sb4). The coordination environment about Sb2 is similar to that about Sb1. Sb3 and Sb4 have comparable coordination but also possess one linking polysulfide, coordi-

---

(17) Wendlandt, W. W.; Hecht, H. G. *Reflectance Spectroscopy*; Interscience Publishers: New York, 1966.

(18) Sheldrick, G. M. SHELXS-86. In *Crystallographic Computing 3*; Sheldrick, G. M., Krüger, C., Doddard, R., Eds.; Oxford University Press: Oxford, U.K., 1985; p 175.

(19) *TEXSAN: Single Crystal Structure Analysis Software*, version 1.6b; Molecular Structure Corp.: The Woodlands, TX 77381, 1993.

(20) Sheldrick, G. M. *SHELXTL-PLUS;* Siemens Analytical X-ray Instruments, Inc.: Madison, WI 53719, 1990.

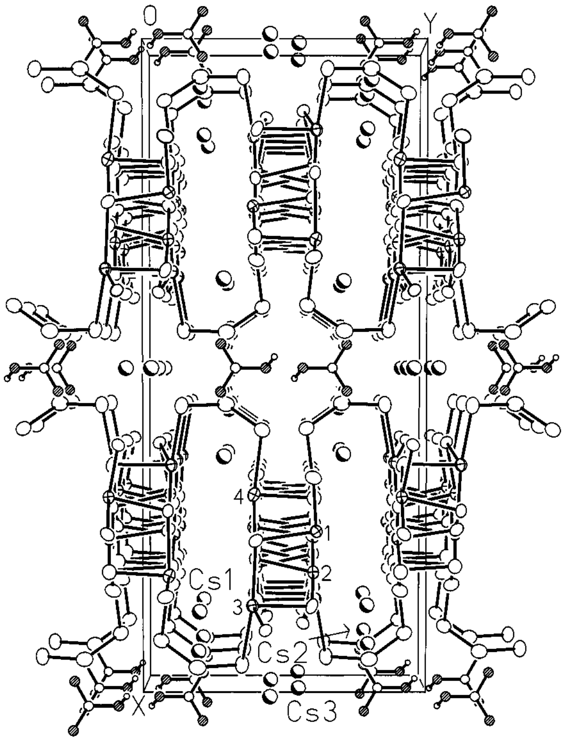

Figure 1. Unit cell view parallel to the *c* axis emphasizing the layered anionic framework, polysulfide chains, and interlayer bicarbonate anions. Cs atoms are highlighted and labeled, Sb atoms are principal ellipsoids with Arabic numerals denoting the crystallographically unique atoms, S atoms are boundary ellipsoids, O atoms are striped spheres, and C and H atoms are open spheres. All ellipsoids are at the 70% probability level.

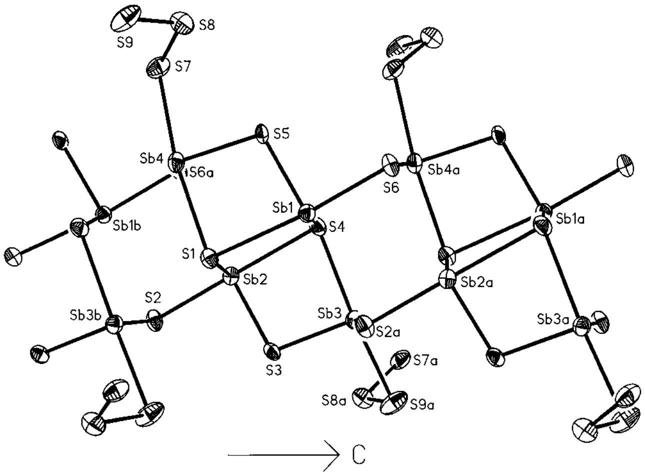

Figure 2. Thermal ellipsoid view of the condensation found in the group 15/16 anionic ribbon as viewed nearly perpendicular to the *c* axis. All ellipsoids are at the 70% probability level.

Table 3. Selected Intramolecular Bond Distances (Å) and Angles (deg) in $Cs_5Sb_8S_{18}(HCO_3)$

Sb1−S1	2.960(6)	Cs1−S1	3.514(6)
Sb1−S4	2.417(7)	Cs1−S2	3.566(6)
Sb1−S5	2.485(6)	Cs1−S4	3.736(6)
Sb1−S6	2.583(5)	Cs1−S5	3.623(7)
Sb2−S1	2.418(6)	Cs1−S6	3.672(6)
Sb2−S2	2.571(6)	Cs1−S7	3.681(6)
Sb2−S3	2.492(6)	Cs1−O1	3.00(2)
Sb2−S4	2.883(5)	Cs2−S2	3.720(7)
Sb3−S2	2.422(6)	Cs2−S3	3.566(6)
Sb3−S3	2.497(6)	Cs2−S5	3.590(6)
Sb3−S4	2.830(6)	Cs2−S6	3.975(6)
Sb3−S9	2.660(8)	Cs2−S7	3.528(7)
Sb4−S1	2.770(6)	Cs2−S8	4.043(6)
Sb4−S5	2.479(5)	Cs2−S8	3.534(7)
Sb4−S6	2.452(7)	Cs2−S9	3.728(7)
Sb4−S7	2.697(7)	Cs2−O1	2.95(2)
S7 −S8	2.039(9)	Cs3−S3	3.486(6) ×2
S8 −S9	2.069(9)	Cs3−S9	3.572(7) ×2
O1−C1	1.31(2) ×2	Cs3−O1	2.95(2) ×2
O2−C1	1.35(4)	O2−H1	0.92
S1−Sb1−S4	84.3(2)	S2−Sb3−S9	92.9(2)
S1−Sb1−S5	84.2(2)	S3−Sb3−S4	89.4(2)
S1−Sb1−S6	174.2(2)	S3−Sb3−S9	95.3(2)
S4−Sb1−S5	94.4(2)	S4−Sb3−S9	172.6(2)
S4−Sb1−S6	93.4(2)	S1−Sb4−S5	88.5(2)
S5−Sb1−S6	90.6(2)	S1−Sb4−S6	90.0(2)
S1−Sb2−S2	92.1(2)	S1−Sb4−S7	169.8(2)
S1−Sb2−S3	93.5(2)	S5−Sb4−S6	99.4(2)
S1−Sb2−S4	86.0(2)	S5−Sb4−S7	84.4(2)
S2−Sb2−S3	90.8(2)	S6−Sb4−S7	84.0(2)
S2−Sb2−S4	177.8(2)	S7−S8−S9	109.7(4)
S3−Sb2−S4	88.3(2)	O1−C1−O1	120.(3)
S2−Sb3−S3	89.9(2)	O1−C1−O2	119.(2)
S2−Sb3−S4	92.9(2)	C1−O2−H1	102.0

nated in an apical position. This complicated bridging pattern creates infinite one-dimensional Sb_4S_6 ribbons which are linked together by the bridging S_3^{2-} chains. This causes the ribbons to stack side by side, creating a two-dimensional layer. The trisulfide bridges also create voids within the layers, between the ribbons, which contain cesium cations (*vide infra*).

The shortest Sb−S bond distances (2.418(6)−2.497(6) Å) are located in the equatorial plane of the trigonal bipyramids, and the longest Sb−S bond distances (2.830(6)−2.960(6) Å) are apical coordination sites, a general trend which has been observed previously.[3,4,7] Within the ψ-SbS_4 units, the axial S−Sb−S bond angles range from 169.8(2) to 177.8(2)°, the equatorial S−Sb−S bond angles vary from 89.9(2) to 99.4(2)°, and the bond angles between apical and equatorial sulfur atoms range from 84.0(2) to 95.3(2)°. The decrease in the equatorial bond angles from the ideal 120° indicates the presence of the lone pair occupying the fifth coordination site on Sb(III). The condensation of the ψ-SbS_4 units is oriented so that all the lone pairs on the antimony atoms point toward the open cavities between the ribbons. This void has a cross-sectional area of 3 Å by 10 Å in the *xy* plane (Figure 1). The nearest Sb−Sb distance across the cavity is 3.558(2) Å; however, the lone pairs of these antimony atoms are not pointed directly at each other, thus relieving any repulsive interaction. The S_3^{2-} chains possess typical S−S single-bond distances and angles (2.039(9) Å, 2.069(9) Å, and 109.7(4)°). Relevant bond distances and angles are given in Table 3.

There are three crystallographically unique cesium cations, one located in the cavity between the Sb−S ribbons (Cs1), one positioned between the S_3 chains (Cs2), and one residing between the layers (Cs3), as seen in Figures 1 and 3. The two cations located within the void space of the layers have an irregular coordination sphere consisting of six sulfur atoms and one oxygen atom, from the bicarbonate. The cesium cation located between the layers is only six-coordinate, to four sulfur and two oxygen atoms, arranged in a bicapped tetrahedral manner. This low coordination number for Cs3 may explain its rather large thermal motion. All Cs−S bond distances range from 3.514(6) to 4.043(6) Å, typical of ionic Cs−S contacts. Unexpectedly, the Cs−O bond distances in the title phase are quite short (2.95(2)−3.00(2) Å) as compared to similar bonds in $CsHCO_3$ which range from 3.122 to 3.752 Å.[21] This may be the result of fewer Cs^+ contacts to the HCO_3^- in the title phase as compared to $CsHCO_3$ or may be due to positional disorder of the bicarbonate anion in the title phase (*vide infra*).

---

(21) Kaduk, J. A. *Z. Kristallogr.* **1993**, *205*, 319.

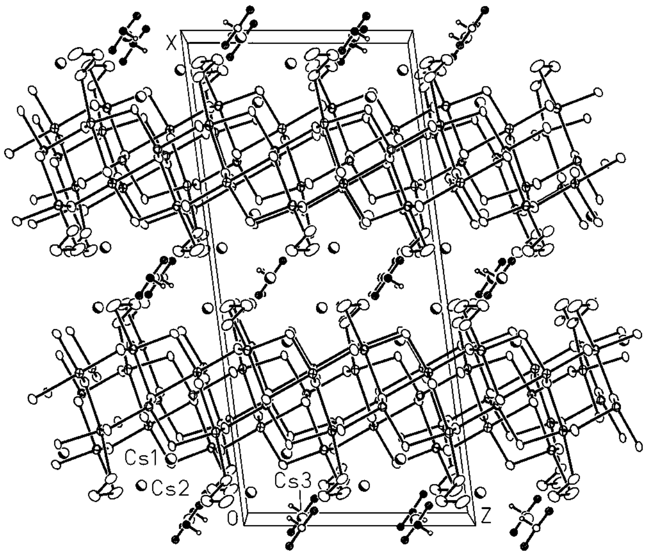

Figure 3. Unit cell view parallel to the *b* axis indicating the location of the cesium atoms. The labeling scheme is the same as in Figure 1.

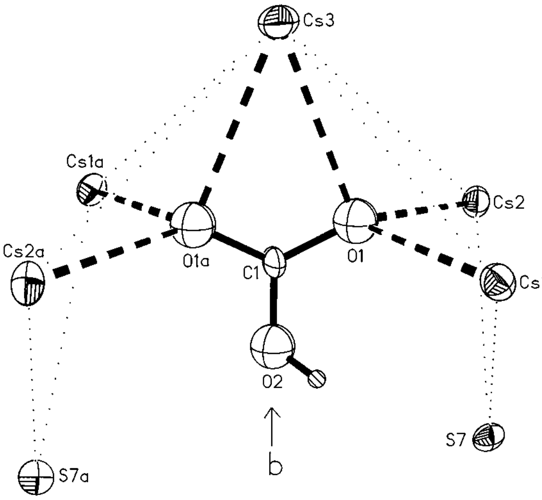

Figure 4. Coordination environment of the bicarbonate anion. Dotted lines denote the coordination sphere about the anion, and dashed lines indicate actual cation−oxygen bonding. All ellipsoids are at the 70% probability level.

The bicarbonate anion located between the antimony sulfide layers is found in an unusually unhindered coordination environment. Crystallographically, C1 resides on a 2-fold rotation axis and O2 is disordered about that rotation axis. While O1 atoms are coordinated to each of the three unique cesium cations (Figure 4), O2 has no contacts to cesium or sulfur atoms less than 3.6 Å. Also, there is no hydrogen bonding, in that oxygen atoms on neighboring bicarbonates are at least 5.6 Å apart. This minimal bonding and disorder observed for O2 may explain the inability to refine even an isotropic temperature factor.

The disordered O2 generates a nonplanar CO_3 fragment; however, attempts to refine C1 off the rotation axis, to achieve planarity, were unsuccessful. This behavior suggests that the anion is exhibiting a wagging motion. The Cs−O1 interactions are short enough to exclude the presence of hydrogen on O1. This observation and the open coordination around O2 imply that a disordered hydrogen is likely present and bonded to O2. After the refinement of the CO_3 fragment, the largest peak in the Fourier difference map did correspond to a reasonable O−H distance (0.92 Å) and C−O−H angle (102°) and thus was included in the refinement as a fixed atom with half-occupancy, due to the disorder imposed by the 2-fold rotation axis. The carbon−oxygen bond distances, 1.31(2) and 1.35(4) Å, are reasonable for a bicarbonate anion. In cesium bicarbonate, these distances range from 1.25 to 1.32 Å.[21]

Discussion

The formation of $Cs_5Sb_8S_{18}(HCO_3)$ appears to be facilitated by the conditions present in supercritical NH_3. The title phase can be prepared as a microcrystalline powder from either Cs_2CO_3 or $CsHCO_3$ in supercritical NH_3. The original source of bicarbonate is open to question. The proton could be derived from the ammonia or, more likely, from adventitious water scavenged from hygroscopic cesium carbonate. The product can be prepared in nearly quantitative yield as a microcrystalline powder. It appears to be stable toward moisture and oxygen. Addition of copper metal does not result in the incorporation of copper but rather leads to single crystals of the product.

As formulated, $Cs_5Sb_8S_{18}(HCO_3)$ is charge-balanced. On the basis of the diffuse-reflectance measurements, the title phase exhibits a linear (absorption)^2 versus energy curve near the absorption edge (2.2−2.6 eV; correlation coefficient = 0.995). This relationship is indicative of materials with direct bandgaps.[22] Therefore, the bandgap can be derived by extrapolating the linear portion of the absorption edge to $(\alpha/s)^2 = 0$ where $h\nu \approx E_g$. This method indicates a bandgap of 2.1 eV, implying semiconducting behavior and thus a charge-balanced system. This result is in agreement with the red-brown color of the compound.

The presence of bicarbonate cannot be conclusively shown via elemental analyses since the relative abundance of carbon and hydrogen is very small. However, infrared spectroscopy did reveal a reasonably sharp band at 3142 cm^{-1}, ν(O−H), that could not be attributed to adventitious water. Also, carbonate bands usually occur at 1400−1500 and 850−900 cm^{-1}, due to symmetric and asymmetric C−O stretches, respectively.[23] However, bicarbonates normally exhibit strong bands around 1000 cm^{-1}, due to C−O−H distortions,[24] as well as bands between 600 and 700 cm^{-1}.[25] The title compound contains bands at 1126 and 996 cm^{-1} and an envelope around 659 cm^{-1}, suggesting the presence of bicarbonate, rather than carbonate. Magnetic susceptibility measurements indicate that the title phase does exhibit paramagnetic behavior. However, standard treatment of the data indicate that the paramagnetic component does not exhibit classical Curie−Weiss behavior. Thus it is presumed that a paramagnetic impurity was present.

The differential scanning calorimetric thermogram shows four endotherms and one exotherm (Figure 5). Loss of adsorbed water occurs at about 375 K, and a broad endotherm starting at approximately 425 K may correspond to the breaking of reactive bonds, possibly the S−S linkages or decomposition of the bicarbonate. On the basis of the powder X-ray diffraction pattern of the product after heating, the exotherm at 500 K is most likely the result of the formation of Sb_2S_3 and Cs_2S. The large and shallow endotherms around 600 K might be due to the subsequent formation of an as yet unknown ternary Cs−Sb−S phase, which would likely be amorphous at this relatively low temperature.

---

(22) Pankove, J. I. *Optical Processes in Semiconductors*; Prentice Hall, Inc.: Englewood Cliffs, NJ, 1971.

(23) Nakamoto, K. *Infrared and Raman Spectra of Inorganic and Coordination Compounds*, 4th ed.; John Wiley and Sons: New York, 1986.

(24) Fischmiester, I. *Spectrochim. Acta* **1964**, *20*, 1071.

(25) Nyquist, R. A.; Kagel, R. O. *Infrared Spectra of Inorganic Compounds*; Academic Press: New York, 1971.

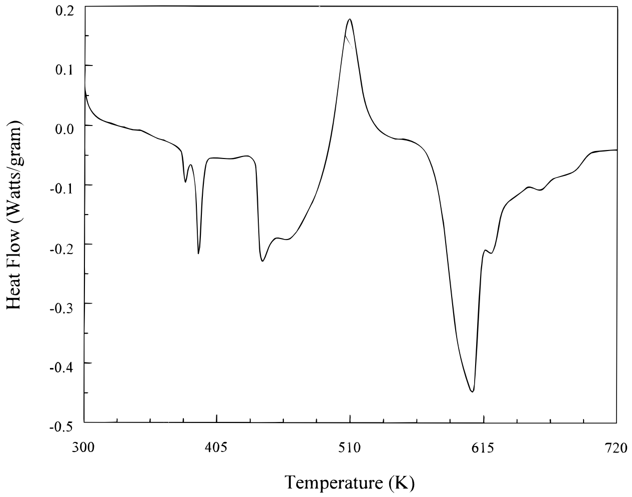

Figure 5. Differential scanning calorimetric thermogram of $Cs_5Sb_8S_{18}(HCO_3)$.

The well-known empirical relationships between bond length and bond valence[26] were utilized to provide insight into the formal valence of the atoms in $Cs_5Sb_8S_{18}(HCO_3)$ (Table 4). For the most part, the calculations indicate that all the cesium cations are monovalent, antimony atoms are trivalent, and the sulfur atoms are divalent. However, the valence of S3 is anomalously high and appears to be due to the extra cationic contact to Cs2, which also has a higher than expected valence sum. The carbon, O1, and O2 valences are within the expected range. For comparison, the three unique oxygen atoms in cesium bicarbonate have bond valences of 1.98, 1.65, and 1.54, which are somewhat lower than those observed in the title phase. This is probably due to significant hydrogen bonding in $CsHCO_3$, which is not possible in $Cs_5Sb_8S_{18}(HCO_3)$. In both cases, the proton was found to reside on the oxygen atom with the lowest bond valence, although the contribution from the proton was not included in the calculations for $CsHCO_3$.

Table 4. Bond Valence Sums for $Cs_5Sb_8S_{18}(HCO_3)$[a]

	Cs	Sb	S	O	C
atom 1	1.12(3)	3.15(5)	2.09(3)	2.16(12)	3.59(25)
atom 2	1.32(3)	3.22(5)	2.22(4)	2.01(11)	
atom 3	1.27(4)	3.08(5)	2.51(4)		
atom 4		3.04(5)	1.99(3)		
atom 5			2.28(3)		
atom 6			2.00(3)		
atom 7			1.88(4)		
atom 8			2.17(5)		
atom 9			1.99(4)		

[a] $\sum s(\mathrm{M-L}) = \sum \exp[(r_0 - r)/0.37]$. s = individual bond valences, r = bond distance in structure, and r_0 = empirically derived M−L single-bond distance (Cs−S = 2.928, Cs−O = 2.417, Sb−S = 2.474, S−S = 2.04, C−O = 1.390, O−H = 0.882 Å). All cation−anion distances are from a table in ref 26, except Cs−S, which was calculated using the formula found in the same reference.

In conclusion, we have reported a new two-dimensional member of the Cs−Sb−S system which is unique because of the presence of bicarbonate anions between the layers. The nature of the interstitial anion cannot be confirmed unambiguously, but crystallography and diffuse-reflectance and IR spectroscopic measurements strongly suggest that it is bicarbonate, rather than carbonate, with the hydrogen source probably derived from adventitious water.

Acknowledgment. We thank Shane J. Hilsenbeck (Iowa State University) for the FTIR spectroscopy, William T. Pennington for insightful crystallographic discussions, and Charles O'Connor (University of New Orleans) for the magnetic susceptibility measurements. This work was supported by the National Science Foundation (Grant CHE-9102548) and the Petroleum Research Fund, administered by the American Chemical Society.

Supporting Information Available: Tables of crystallographic and refinement details, anisotropic thermal parameters, and bond angles, as well as text giving further structural details supporting the formulation of the interstitial anion as bicarbonate (5 pages). Ordering information is given on any current masthead page.

IC960359H

---

(26) Brown, I. D.; Altermatt, D. *Acta Crystallogr.* **1985**, *B41*, 244.